IOPscience iopscience.iop.org

Home Search Collections Journals About Contact us My IOPscience

Properties of non-equivalent sites and bandgap of spinel-phase silicon nitride

This article has been downloaded from IOPscience. Please scroll down to see the full text article.

2004 J. Phys.: Condens. Matter 16 6469

(http://iopscience.iop.org/0953-8984/16/36/012)

View the table of contents for this issue, or go to the journal homepage for more

Download details:
IP Address: 129.252.86.83
The article was downloaded on 27/05/2010 at 17:26

Please note that terms and conditions apply.

J. Phys.: Condens. Matter **16** (2004) 6469–6476 PII: S0953-8984(04)81045-2

Properties of non-equivalent sites and bandgap of spinel-phase silicon nitride

S Leitch[1], A Moewes[1], L Ouyang[2], W Y Ching[2] and T Sekine[3]

[1] Department of Physics and Engineering Physics, University of Saskatchewan, 116 Science Place, Saskatoon, SK, S7N 5E2, Canada
[2] Department of Physics, University of Missouri-Kansas City, Kansas City, MO 64110, USA
[3] National Institute for Materials Science, Namiki, 1-1, Tsukuba 305-0044, Japan

Received 20 May 2004
Published 27 August 2004
Online at stacks.iop.org/JPhysCM/16/6469
doi:10.1088/0953-8984/16/36/012

Abstract

γ-Si_3N_4 is a nitrogen-based ultra-hard ceramic with Si atoms occupying both tetrahedral and octahedral sites in a spinel structure. Soft-x-ray emission and absorption spectra of γ-Si_3N_4 are presented, which together provide an experimentally determined bandgap of 4.30 ± 0.25 eV. Information about localized partial density of states (LPDOS) of the non-equivalent Si sites is presented.

The spinel phase of Si_3N_4 (γ-Si_3N_4) is the third synthesized phase of silicon nitride. It is characterized by a cubic spinel structure, with Si atoms occupying both tetrahedral (t-Si) and octahedral (o-Si) sites. Originally synthesized by Zerr *et al* [1], γ-Si_3N_4 is the first nitride ceramic to exhibit octahedrally coordinated Si. This discovery introduced the possibility of other nitride ceramics that could be synthesized in this spinel structure [2–4].

Increased hardness, thermal stability and resistance to oxidation [5–8] make γ-Si_3N_4 an important material for structural and mechanical applications. In addition, first-principles calculations [4] have predicted γ-Si_3N_4 to be a large-gap semiconductor, with a direct bandgap of 3.45 eV. Further calculations have suggested that this gap can be tuned by doping the material [9]. Preliminary measurements performed by Zerr *et al* have suggested a bandgap of 3.3 eV [10]. A bandgap in this range provides the potential for this material to be used in light emitting electronics and semiconductor power devices. Single crystals of sufficient size have yet to be synthesized, and therefore conventional methods of verifying the bandgap by optical means are not feasible. Measuring the bandgap, as well as insight into the unique properties of the non-equivalent octahedral and tetrahedral Si sites, are the motivations for this paper.

γ-Si_3N_4 powder was synthesized from β-Si_3N_4 by the shock compression method [11] and purified by a hot hydrofluoric acid solution [12]. The powder has been characterized using x-ray diffraction, differential thermal analysis [13] and 29-Si magic-angle-spinning NMR [14].

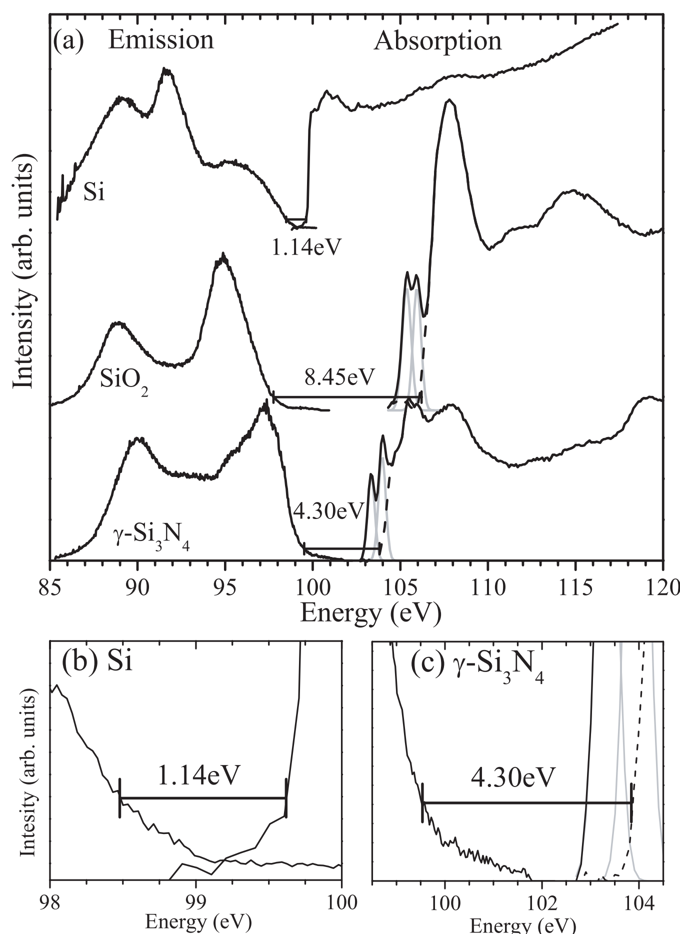

Figure 1. (a) Si $L_{2,3}$ absorption and emission for SiO_2, crystalline Si, and γ-Si_3N_4. Absorption was taken using the total fluorescence yield (TFY). The bandgap for Si_3N_4 can be directly measured from these data. Expanded views of the onset edges have been included for (b) Si and (c) γ-Si_3N_4.

The oxygen content of the purified γ-Si_3N_4 has been determined to be 2.0 wt% by a high-temperature combustion method in the LECO Co. furnace. Therefore, the γ-Si_3N_4 powder is considered to consist of pure nitride spinel phase.

X-ray absorption and emission spectroscopy (XAS and XES) were used to probe the localized partial density of occupied and unoccupied states (LPDOS) near the Fermi level. A powdered sample of γ-Si_3N_4 was measured under ultra-high-vacuum conditions (5×10^{-9} Torr) and room temperature at beamline 8.0.1 of the Advanced Light Source at the Lawrence Berkeley National Laboratory [15].

The measured XAS spectra for the Si $L_{2,3}$ transition of crystalline Si, SiO_2, and γ-Si_3N_4 are shown on the right side of figure 1. It is known that Si $L_{2,3}$ absorption is dominated by broadening due to the short lifetime of intermediate states. For all XAS measurements, the experimental resolution due to the monochromator is 0.02 eV. The Si spectrum (top) shows an absorption edge at 99 eV, in agreement with previous measurements [16]. The SiO_2 spectrum (middle) has a double peak at ~105.5 eV that originates from excitonic states situated in the

bandgap. The double peak of SiO_2 is considered to be due to spin–orbit interactions in the $L_{2,3}$ transition with a peak separation of 0.6 eV. The sharp peak at 107.5 eV is due to the onset of conduction band absorption. γ-Si_3N_4 (bottom) also shows two pre-threshold peaks from promotion to excitonic states. We conclude this by observing the 0.6 eV peak separation, which is similar to the L_2–L_3 spin–orbit energy difference, as well as the sharp nature of the peaks, which is characteristic of absorption to excitonic states. The near-edge peaks also exhibit selective excitation of the two non-equivalent sites, which is discussed in more detail later in the paper. Above threshold, γ-Si_3N_4 shows a more complex structure than SiO_2, α-Si_3N_4, and β-Si_3N_4 [17, 18]. This is due to the sixfold bonding of Si, and the increased complexity of the added octahedral bonding. Our absorption spectrum shows good agreement with a recent electron loss near-edge spectral (ELNES) measurement [19].

The measured non-resonant XES spectra for the Si $L_{2,3}$ transition of the three materials are shown on the left side of figure 1. Si $L_{2,3}$ emission spectra are dominated by lifetime broadening of the valence band hole. This final state effect is $\sim$3 eV [20], which is much larger than the experimental resolution for all XES measurements of 0.1 eV. Si (top) has a low-energy peak due to non-bonded valence band 3s states, a sharper peak at 92 eV due to 3s symmetry in the s–p hybridized bonding states and a broad peak above 94 eV resulting from p states showing d character [21]. The SiO_2 emission spectrum (middle) has two peaks and is also consistent with previous measurements [22]. For the emission spectrum of γ-Si_3N_4 (bottom), the highest-energy occupied LPDOS of γ-Si_3N_4 has a higher energy than Si and SiO_2. γ-Si_3N_4 has two main peaks, with a shoulder appearing near the high-energy peak. The lowest-energy peak, near 90 eV, is due to 3s symmetry in occupied o-Si states, and a mixer of 3s and 3d symmetry in t-Si states. The high-energy peak ($\sim$97 eV) is a result of bonding states showing 3d symmetry of o-Si states, with t-Si 3d symmetric bonding states causing the low-energy shoulder. The region between the two main peaks is relatively flat, and is attributed to a mixture of 3s and 3d symmetry of states from both sites.

Absorption and emission spectra in figure 1 are shown on the same energy scale to facilitate measurement of the bandgap. Since the excitonic peaks of SiO_2 and γ-Si_3N_4 do not contribute to the bandgap measurement, they have been fitted to Gaussians of equal width and subtracted from the bulk of the spectra. The onset energies are then found by extending the spectral onset slope to the noise floor. Figures 1(b) and (c) show a close-up view of the onset region for Si and γ-Si_3N_4. For the absorption edges, the onset slope is steep, so the onset energy can be found directly by observation. The small tail produced by instrumental broadening is ignored. The onset energy for emission is determined by drawing a line along the slope of the onset and along the slope of the noise floor. The point where these two lines cross is the onset energy. Again, the tail produced by instrumental broadening is ignored. The error for each measurement is defined by the ability to accurately measure the onset energy. Using this method, crystalline Si has a bandgap of $1.1(4) \pm 0.10$ eV, in excellent agreement with the well established value. The adjusted spectra for SiO_2 reveal a bandgap of 8.45 ± 0.30 eV. This value has been debated in the literature [23], but can be considered a reasonable value. Finally, the experimentally determined bandgap of γ-Si_3N_4, after compensating for excitonic states, is 4.30 ± 0.25 eV.

In our approach, the use of reference spectra is very important for bandgap measurements using XAS and XES, since the measured value can be complicated by a number of factors. The LPDOS of the final state in absorption will be altered due to the presence of the core hole. The core hole causes the onset of the absorption spectra to shift to lower energies compared to the valence band, which will decrease the bandgap by $\sim$0.5 eV in γ-Si_3N_4. Spin–orbit interactions produce two nearly identical overlapping spectra, one for the L_2 transition and one for the L_3 transition with a separation of 0.5 eV for γ-Si_3N_4. The overlapped spectra will

therefore effectively reduce the measured bandgap by a factor of 0.5 eV. The polycrystalline particle size of γ-Si_3N_4 reaches the nanometre scale, where quantum confinement effects become apparent. Studies of quantum confinement in Si nano-particles show that the valence band edge migrates to lower energies, which effectively increases the bandgap. The shifts in valence and conduction bands as a function of particle size for Si nano-particles were studied and a bandgap widening of 0.26 eV (VB: −0.2 eV, CB: +0.06 eV) for 3.2 nm Si particles compared to crystalline Si was found [16]. Extrapolating these data, we estimate a maximum total shift of VB and CB edges of much less than 0.2 eV (for particles of 10 nm size) for our 10–50 nm γ-Si_3N_4 particles. Also, phonon effects in polar materials have been found to cause spectral broadening, as well as a shift of the occupied states to lower energies [24]. This effect is most apparent in ionically bonded SiO_2, but nearly zero in covalently bonded Si. Since γ-Si_3N_4 is a strongly covalently bonded material, the effects of phonon interactions will also be minimal. The bandgap measurements for two known samples, crystalline Si and α-quartz (SiO_2), are included to verify our method is appropriate.

Understanding the LPDOS differences of t-Si and o-Si in γ-Si_3N_4 is important to understand the electronic properties of the material. In principle, one could attempt to extract site-specific information based on geometry using angular-resolved photo-emission spectroscopy (ARPES). However, ARPES only measures the total density of states and requires a single crystal with known orientation. All synthesized γ-Si_3N_4 to date is polycrystalline, with small (10–50 nm) crystal grains [11], and therefore cannot currently be measured using ARPES. LPDOS properties of the non-equivalent sites can be determined using XAS and XES, by exploiting site-specific absorption of the material, as previously demonstrated by Guo *et al* [25]. Excitation of an electron in one non-equivalent Si site will produce emission from only that site. The emission spectrum will consequently exhibit features unique to that non-equivalent site. The challenge is to efficiently excite core electrons from one non-equivalent site, while minimizing the excitation of others. We accomplish this by comparing the XAS spectrum with site-specific x-ray absorption near-edge spectra (XANES) calculations that include matrix elements and the effect of the core hole [26].

Figure 2 shows the absorption spectrum for γ-Si_3N_4, as well as calculated Si $L_{2,3}$ XANES. Discounting the excitonic peaks, the calculated total XANES shows good agreement with the experimental data. The total XANES is obtained by a weighted average of the bottom two XANES spectra, which are the contribution from each non-equivalent site. The weighting is based on a 2:1 octahedral-to-tetrahedral site density. Arrows mark the features of the XAS spectrum corresponding to the excitation energies used for XES, chosen based on high absorption probability, and a significant difference between the two site-specific XANES.

Figure 3 shows the XES emission spectra, as well as calculated LPDOS for o-Si and t-Si states with s and d symmetry below the Fermi level. The calculated LPDOS does not include core-hole effects, since ground-state LPDOS gives a more accurate representation of the emission spectra, which one would expect taking into account the final state rule. The o-Si LPDOS has been shifted 0.6 eV lower in energy with respect to t-Si LPDOS to account for the transition energy of each site. All of the spectra are renormalized, so that the intensities are equivalent at 91 eV, where the site-specific LPDOS differences are minimal.

As mentioned previously, the method of analysing non-equivalent sites is similar to one used on $La_{2-x}Sr_xCuO_4$ by Guo *et al* [25]. However, unlike $La_{2-x}Sr_xCuO_4$, which has very strong spectral differences from two non-equivalent oxygen sites, there is very little spectral dispersion observed in γ-Si_3N_4 due to the broad nature of Si absorption and emission spectra caused by strong lifetime broadening. Broad features in the absorption spectra reduce the ability to uniquely excite each non-equivalent site while broadening of the emission spectra reduces the ability to assign spectral differences to non-equivalent sites. Only emission from

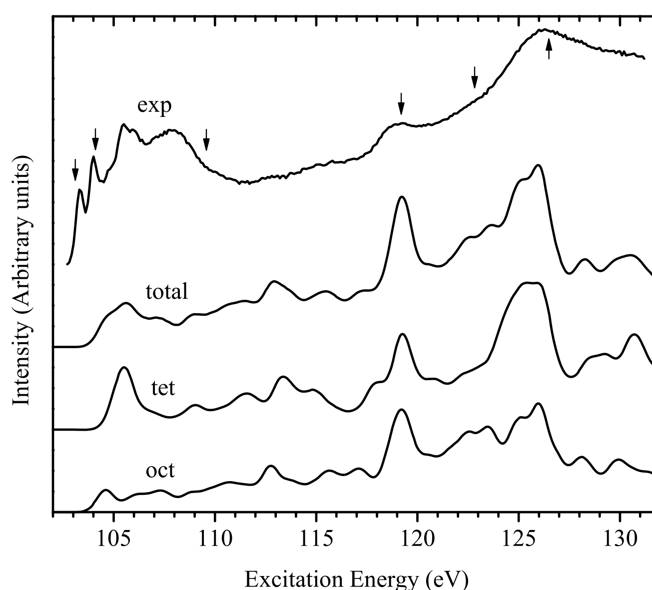

Figure 2. Si $L_{2,3}$ XAS measured (top), with calculated, site-selective XANES (bottom). Arrows mark the features of the XAS spectrum corresponding to the excitation energies used for XES.

the sharp excitonic peaks, at 103.3 and 104.1 eV, shows a measurable difference. We note that if the two sharp absorption features (at 103.3 and 104.1 eV in figure 2) discussed above were due to spin–orbit splitting alone, one would expect the emission spectra excited at these two energies to be identical in shape but shifted by 0.5 eV, which is not the case. RIXS effects are also known to cause dispersion for near-edge emission. However, by comparing the calculated LDPOS for each non-equivalent site with these spectra, similarities are apparent, which therefore supports our interpretation of the two sharp absorption features exhibiting a site-selective process. In order to visualize the small non-equivalent site differences in more detail, we compare difference spectra.

Figure 4 shows the difference spectra of the two excitonic emission spectra, two non-excitonic emission spectra (excited at 110.0 and 119.2 eV), and the difference spectra for the calculated LPDOS of the non-equivalent sites in figure 2. Pairs of spectra were chosen to represent o-Si and t-Si emission respectively. The spectrum showing predominantly t-Si emission ($h\nu_{exc} = 104.1$ and 110.0 eV) was subtracted from the spectrum showing predominantly o-Si emission ($h\nu_{exc} = 103.3$ and 119.2 eV). Since the spectra were normalized to a point where the LPDOS differences were minimal, the difference spectra show the relative intensity of emission from each non-equivalent site. We determine site-specific information by comparing the experimentally derived difference spectra with the calculated LPDOS difference spectra.

The difference spectrum for the two non-excitonic emission spectra (figure 4(c)) provides little insight into the unique properties of the non-equivalent sites. Although some structure can be seen, there is not enough difference to draw a reasonable conclusion. The difference spectrum from excitation at the two excitonic peaks (figure 4(b)) shows a measurable difference, which is compared with the site-specific LPDOS difference (figure 4(a)). The high-energy onset of t-Si is at a higher energy than o-Si, producing a negative peak at 98.5 eV. The rest of the spectrum is dominated by o-Si emission, seen as two positive peaks at 97.5 and 89.5 eV.

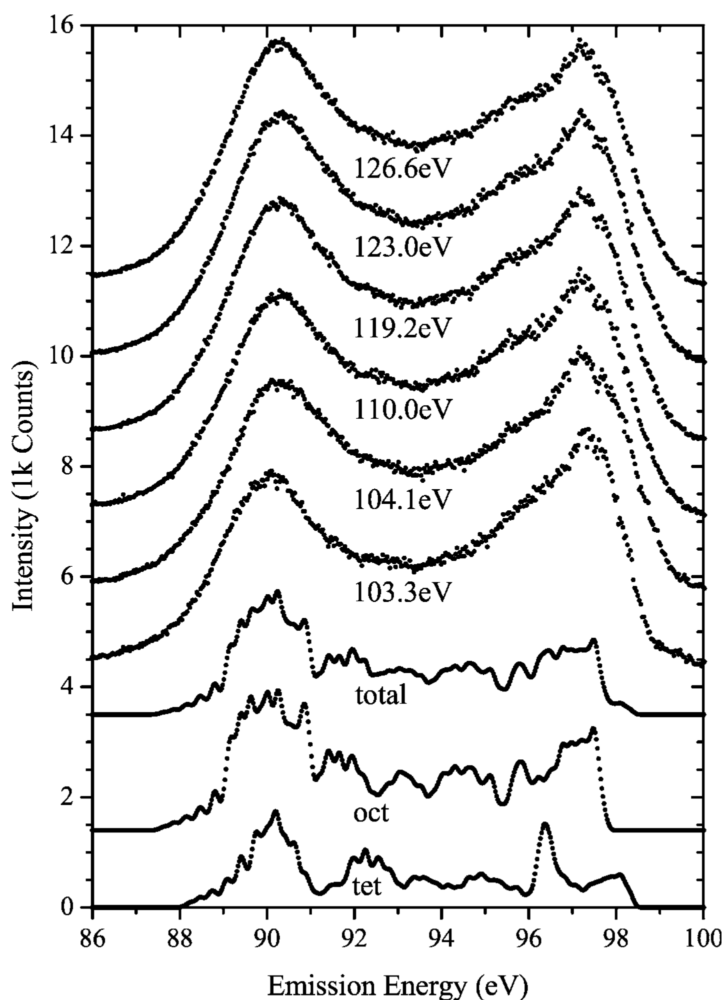

Figure 3. Si $L_{2,3}$ XES data measured for γ-Si_3N_4 (top). The excitation energy used for each measurement is displayed below. Peak ratio change is attributed to site-selective LPDOS of Si (bottom).

A feature appears in the high-energy peak at 97 eV, and is due to a peak in 3d t-Si LPDOS. Close agreement between the experimental and calculated difference spectra provides strong evidence that properties of individual non-equivalent sites can be obtained experimentally.

We note that the idea of analysing difference spectra of XES and comparing to DOS difference spectra requires the presence of a brilliant third-generation synchrotron source overcoming the otherwise typical low count rates inherent with soft x-ray emission spectroscopy.

To summarize, XES and XAS spectra have been presented for γ-Si_3N_4, which together provide an experimentally determined bandgap of 4.30 ± 0.25 eV. Non-equivalent Si sites within γ-Si_3N_4 can be analysed using a method that uses site-selective emission from each site. This method of determining site-specific properties provides insight into unique properties of same-element, non-equivalent bonding atoms that is non-destructive, bulk sensitive, and works equally well for single-crystal and polycrystalline samples.

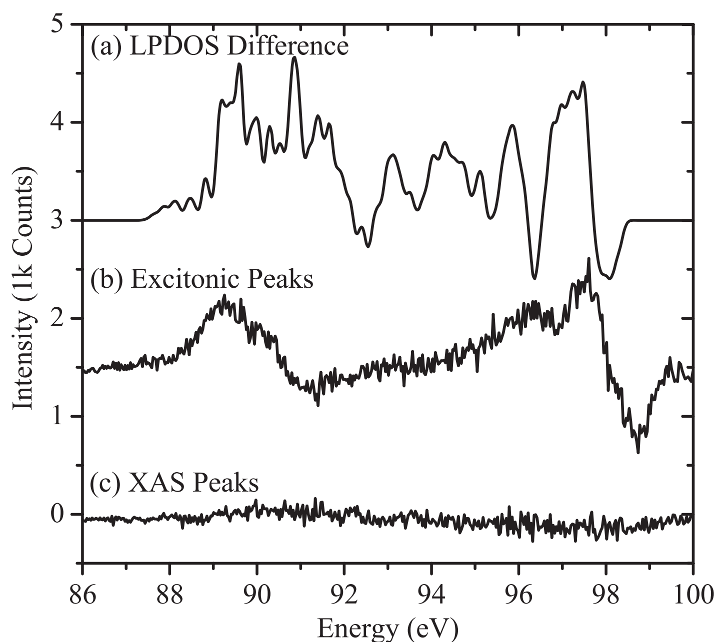

Figure 4. (a) Site-selective LPDOS difference, along with $L_{2,3}$ XES emission difference spectra from (b) excitonic peaks ($h\nu_{exc}$ = 104.1 and 103.3 eV) and (c) XAS peaks ($h\nu_{exc}$ = 110.0 and 119.2 eV).

Acknowledgments

Funding by the Natural Sciences and Engineering Research Council of Canada (NSERC) is gratefully acknowledged. AM is a Canada Research Chair. Work at UMKC is supported by the US Department of Energy (contract No DE-FG02-84DR45170), and an NEDO International grant.

References

[1] Zerr A *et al* 1999 *Nature* **400** 340–2
[2] Ching W Y *et al* 2002 *J. Am. Ceram. Soc.* **85** 75–80
[3] Tanaka I *et al* 2002 *J. Mater. Res.* **17** 731–3
[4] Mo S D *et al* 1999 *Phys. Rev. Lett.* **83** 5046–9
[5] Jiang J Z *et al* 2001 *J. Phys.: Condens. Matter* **13** L515–20
[6] Soignard E *et al* 2001 *J. Phys.: Condens. Matter* **13** 557–63
[7] Jiang J Z *et al* 2002 *Phys. Rev.* B **65** 161202
[8] Zerr A *et al* 2002 *J. Am. Ceram. Soc.* **85** 86–90
[9] Oba F *et al* 2001 *Appl. Phys. Lett.* **78** 1577–9
[10] Zerr A *et al* 2002 *Acta Crystallogr.* A **58** C47
[11] Sekine T *et al* 2000 *Appl. Phys. Lett.* **76** 3706–8
[12] Sekine T 2002 *J. Am. Ceram. Soc.* **85** 113–6
[13] Sekine T and Mitsuhashi T 2001 *Appl. Phys. Lett.* **79** 2719–21
[14] Sekine T, Tansho M and Kanzaki M 2001 *Appl. Phys. Lett.* **78** 3050–1
[15] Jia J J *et al* 1995 *Rev. Sci. Instrum.* **66** 1394–7
[16] van Buuren T *et al* 1998 *Phys. Rev. Lett.* **80** 3803–6
[17] Nithianandam V J and Schnatterly S E 1987 *Phys. Rev.* B **36** 1159–67
[18] Ching W Y, Mo S D and Chen Y 2002 *J. Am. Ceram. Soc.* **85** 11–5

[19] Tanaka I *et al* 2001 *Appl. Phys. Lett.* **78** 2134–6
[20] Eisebitt S 1994 *PhD Thesis* Kernforschungszentrum Jülich
[21] Rubensson J E *et al* 1990 *Phys. Rev. Lett.* **64** 1047–50
[22] Nithianandam V J and Schnatterly S E 1988 *Phys. Rev.* B **38** 5547–53
[23] Weinberg Z A, Rubloff G W and Bassous E 1979 *Phys. Rev.* B **19** 3107–17
[24] O'brien W L *et al* 1993 *Phys. Rev.* B **47** 140–3
[25] Guo J H *et al* 1994 *Phys. Rev.* B **49** 1376–80
[26] Mo S D and Ching W Y 2000 *Phys. Rev.* B **62** 7901–7